THE JOURNAL OF PHYSICAL CHEMISTRY C

Article

Cite This: J. Phys. Chem. C 2019, 123, 24031−24038

pubs.acs.org/JPCC

Surface-Specific Spectroscopy of Water at a Potentiostatically Controlled Supported Graphene Monolayer

L. B. Dreier,[†,‡] Z. Liu,[†,#] A. Narita,[†] M.-J. van Zadel,[†] K. Müllen,[†,§] K.-J. Tielrooij,[∥] E. H. G. Backus,[†,⊥] and M. Bonn*[,†]

[†]Max Planck Institute for Polymer Research, Ackermannweg 10, 55128 Mainz, Germany

[‡]Graduate School Materials Science in Mainz, Staudingerweg 9, 55128 Mainz, Germany

[§]Institute of Physical Chemistry, Johannes Gutenberg-Universität Mainz, Duesbergweg 10−14, 55128 Mainz, Germany

[∥]Catalan Institute of Nanoscience and Nanotechnology (ICN2), CSIC and BIST, Campus UAB, Bellaterra, 08193 Barcelona, Spain

[⊥]Department of Physical Chemistry, University of Vienna, Währinger Strasse 42, 1090 Vienna, Austria

ABSTRACT: Knowledge of the structure of interfacial water molecules at electrified solid materials is the first step toward a better understanding of important processes at such surfaces, in, e.g., electrochemistry, atmospheric chemistry, and membrane biophysics. As graphene is an interesting material with multiple potential applications such as in transistors or sensors, we specifically investigate the graphene−water interface. We use sum-frequency generation spectroscopy to investigate the pH- and potential-dependence of the interfacial water structure in contact with a chemical vapor deposited (CVD) grown graphene surface. Our results show that the SFG signal from the interfacial water molecules at the graphene layer is dominated by the underlying substrate and that there are water molecules between the graphene and the (hydrophilic) supporting substrate.

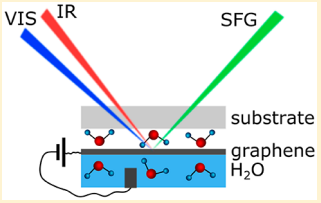

INTRODUCTION

Due to the importance of the graphene−water interactions in various technological applications, it is of great interest to improve our understanding of the water structure at the graphene−water interface. For example, it has been shown that nanoporous graphene can be used for desalination of water[1] and in electricity generation devices.[2] Furthermore, as the electronic properties of graphene are changed by its interaction with water, the resistance of graphene-based transistors and sensors varies with a change in humidity.[3] Despite substantial previous research on graphene in contact with water during the last decades, many open questions remain. For instance, there is still no scientific consensus regarding the wettability of graphene, one of the most fundamental properties of the graphene−water interface. The reported water contact angles for graphene range from 20° to 127°.[4,5] These variations are often attributed to chemical doping or substrate effects.[6−8] Given that materials with a water contact angle below (above) 90° are defined as hydrophilic (hydrophobic),[9] this implies that it is debated whether graphene is hydrophilic or hydrophobic.

Given its outstanding conductive nature, graphene further provides a unique opportunity. Graphene can be charged at will and can thus be used to probe changes in the water structure as a function of an applied external potential. Aqueous solutions are often in contact with charged, solid surfaces. Examples include water at charged mineral surfaces,[10] in riverbeds, or in technologically relevant processes such as in catalysis[11] and electrochemistry.[12] The surface charge of these solid surfaces greatly influences the interfacial water structure, as the water molecules are aligned by the field arising from the charge at the interface.[13] Since the surface charge changes upon varying the pH or introducing electrolytes, the interfacial water orientation is also altered by these effects.[12,14] Both the effect of pH and electrolyte concentration on the interfacial water structure have already been thoroughly investigated.[15,16] However, altering electrolyte concentration or pH modifies not just the surface charge, but often also the chemistry of the system. Graphene overcomes this limitation, as applying a potential induces purely physical changes at the interface.

Understanding changes in the structure of interfacial water as a function of surface potential at electrified interfaces is not only fundamentally interesting but also highly technologically relevant for electrochemical, electrocatalytic, and biochemical applications.[12] To study the water structure at the interface, sum-frequency generation (SFG) spectroscopy can be used. SFG is a second-order nonlinear optical spectroscopy, which requires symmetry breaking to give a signal. As bulk water is inherently centrosymmetric, a vibrational signal from only the interfacial water molecules is obtained. At a charged surface, the interfacial water molecules are aligned by the charge, resulting in general in a higher order and thus an enhanced SFG signal. To investigate the influence of an applied potential on the interfacial water structure, the SFG signal of water in contact with conductive materials has to be measured. Recently, Campen and co-workers have reported the

Received: June 19, 2019
Revised: September 5, 2019
Published: September 9, 2019

potential-dependent structure of free −OH groups of interfacial water at a gold surface.[17] In their experiment, they direct the laser beams through a thin layer of water to investigate the interface they are interested in. Due to the absorption of IR light by the water molecules, their approach cannot easily be used to investigate the hydrogen-bonded water structure. The interactions of water with gold, ITO, and titanium have also been studied previously.[18] However, the nonresonant contributions to the SFG signal, originating from electronic transitions in the respective solid material, were overwhelming. It was thus not possible to determine the SFG signal from water at the interface. Since graphene is inherently atomically thin,[19] its nonresonant contributions are expected to be substantially reduced. Thus, it should be possible to observe the water vibrations at the water−graphene interface. As graphene is a highly conductive material, the charge carrier density can be changed by applying a voltage. By measuring SFG spectra of the water−graphene interface, while applying a voltage to the graphene layer, we should thus be able to monitor the effect a change in surface potential has on the interfacial water orientation.

METHODS

Graphene Layer Preparation. Chemical vapor deposited (CVD) graphene was grown on copper (Cu) foil in a custom-made hot wall furnace with a sealed quartz tube. After annealing of the Cu foil surface at 1040 °C for 40 min under ultrapure hydrogen gas flow (100 sccm), methane (CH_4) gas flow (25 sccm) was opened for 20 min as carbon source. Samples from commercial sources (Graphenea) were also used. The resulting graphene layer on the Cu foil was subsequently coated with a poly(methyl methacrylate) (PMMA) protecting layer. The Cu was etched away, and the graphene under the PMMA film was transferred onto the desired substrate, either CaF_2 or SiO_2, in water. Finally, the PMMA was removed by immersing it into hot acetone at 55 °C for 30 min, which was repeated for three times. In contrast to previous reports,[20] no PMMA residue was observed with SFG spectroscopy in the vibrational region of the CH stretch mode. However, it is well-known that it is difficult to entirely remove PMMA residues;[21,22] there might thus still be PMMA residue on the samples. Atomic force microscopy (AFM) images show large areas of free graphene and some residue that seems to appear as bright protrusions covering up to a few percent of the surface (see Figure 1a). The clearly visible dark stripes in the AFM image originate from the CaF_2 substrate underneath the graphene layer. In addition to AFM, the transferred graphene layers were further characterized using Raman spectroscopy and optical microscopy. Additionally, the sheet resistance of the graphene film, which typically had a value of ∼1 kΩ/sq, was measured before using it for the experiments. A characteristic Raman spectrum of a graphene layer is shown in Figure 1b. Two spectral features appear in the Raman spectrum at ∼1585 and ∼2690 cm^{-1}, corresponding to the G and 2D band, respectively. The symmetric shape and small full width at half-maximum of up to 40 cm^{-1} of the 2D signal indicates that the sample consists of 1 to 2 layers of graphene.[23] The absence of a defect signal at ∼1350 cm^{-1} shows that there is no significant amount of defects present in the monolayer.[24] Furthermore, one can infer a carrier density in the order of 10^{12} cm^{-2} from the G band position at ∼1585 cm^{-1}.[25,26]

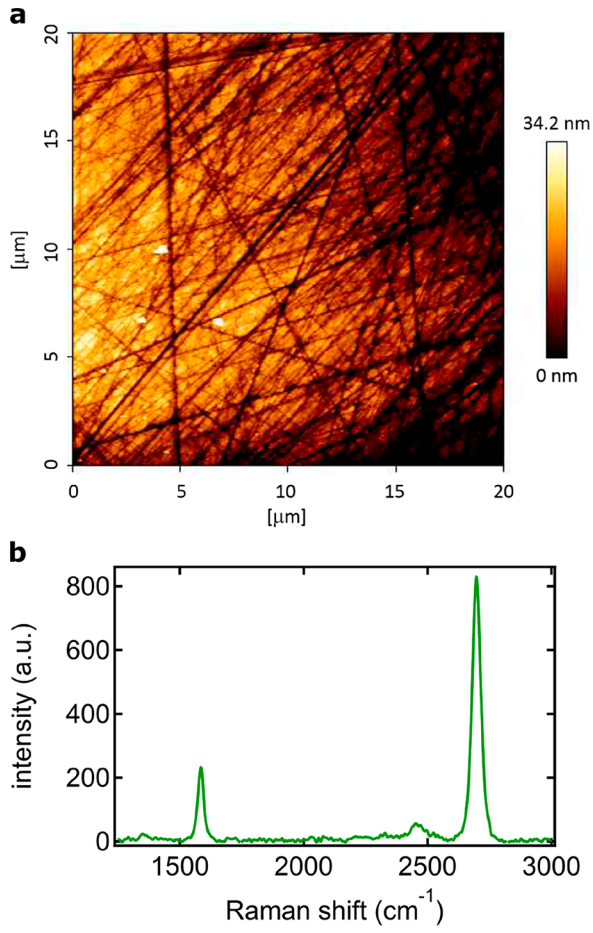

Figure 1. Representative (a) AFM image and (b) Raman spectrum of a graphene layer used for the experiments. The lines in the AFM image originate from the roughness of the CaF_2 substrate, not the graphene.

As the CVD method results in continuous graphene layers, all experiments reported here were performed on this type of graphene. Several other methods, namely depositing electrochemically exfoliated graphene[27] or graphene oxide (GO) via the Langmuir−Blodgett technique as well as spin-coating the GO dispersion, were also tried. However, none of them yielded high-quality, continuous, macroscopically conducting graphene layers.

Design of the Spectro-Electrochemical Cell. A spectro-electrochemical cell was designed for measuring SFG spectra while applying a potential. A schematic of the cell is shown in Figure 2.

The cell mainly consists of three polytetrafluoroethylene (PTFE) parts, labeled "base", "electrolyte chamber", and "clamp ring" in Figure 2a. The base has four small conical holes in the raised center. Two are used as electrolyte inlet and outlet and two are used to hold the counter and reference electrodes (CE and RE). PTFE tubes are pulled through the holes. The conical shape of the holes deforms the PTFE tube to create a watertight seal between base and tube. For the electrolyte in- and outlet, Bola tubes with an inner diameter (ID) of 0.5 mm and an outer diameter (OD) of 1.6 mm were used. Both the electrodes are inside Bola tubes (0.8 mm ID/1.6 mm OD) and are pulled through the holes in the base together with the tubes.

DOI: 10.1021/acs.jpcc.9b05844
J. Phys. Chem. C 2019, 123, 24031−24038

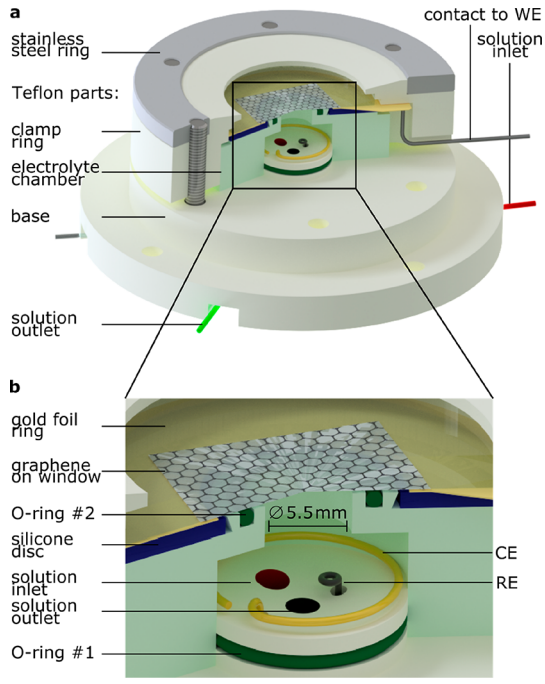

Figure 2. Schematic of the newly designed spectro-electrochemical cell (a) and enhanced image of the electrolyte chamber (b). WE, RE, and CE are the working, reference, and counter electrodes, respectively.

The electrolyte chamber is placed on the base. An O-ring (#1) is used to create a seal between the base and the electrolyte chamber. The bottom of the electrolyte chamber has a diameter of 12 mm to create sufficient electrolyte volume and space for the counter- and reference electrodes. The top of the electrolyte chamber has a diameter of only 5.5 mm. A second O-ring (#2) is needed to create a seal between the electrolyte chamber and the graphene layer (working electrode) on the window. A thin gold foil ring (99.99%, 0.1 mm thickness, Hauner Metallische Werkstoffe) is used as an electrical connection between the graphene working electrode and the potentiostat. The gold foil ring has an inner diameter larger than the outer diameter of O-ring #2 but still small enough to overlap with the graphene layer and create a sufficient contact area between graphene and gold. Once the cell is pressed together, a soft silicone disk (1.75 mm thick, see Figure 2b) on top of the electrolyte chamber is used to press the gold foil ring onto the graphene layer while at the same time a seal is created between the electrolyte chamber and the graphene by O-ring #2. This way, we ensure the gold foil ring is never in contact with the electrolyte and can be biased externally. The cell is pressed together with the clamp ring and stainless steel screws. Since PTFE is very soft, a stainless steel ring with threaded holes is used. A schematic of the spectro-electrochemical measurement setup is shown in Figure 3.

Experimental Procedure. All the parts of the cell and all the glassware used to prepare the solutions were boiled in 40% nitric acid before usage. After cooling down, the cell parts were rinsed with water, while the glassware for the sample preparation was boiled twice in water before being used. The H_2O used for all rinsing steps as well as for boiling the glassware and preparing the electrolyte solutions was deionized with a Millipore unit (resistivity ≥18.2 MΩ cm). The substrate with the graphene on top was only rinsed with water, ethanol,

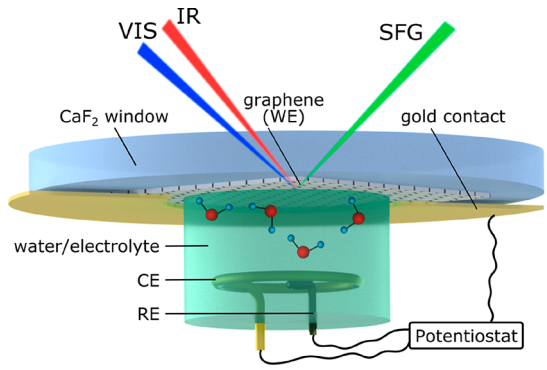

Figure 3. Schematic of the electrochemical measurement setup. WE, RE, and CE are the working, reference, and counter electrodes, respectively.

and again with water. The reference electrode was wrapped around a platinum wire (0.5 mm diameter, 99.997%, Alfa Aesar) that was used as a connection. A gold wire (0.5 mm diameter, 99.95%, Alfa Aesar) was used as a counter electrode. After assembling all parts, the cell was filled with the electrolyte solution by pumping it in using the pressure of argon gas. To achieve a bubble-free filling, the direction of the flow was reversed once or twice during the filling process. After the cell had been filled, the inlet and outlet tubes were connected and wrapped with Parafilm to achieve a watertight system and to avoid air bubbles appearing in the cell.

In the first attempt, Ag/AgCl was used as a reference system. However, in this configuration, we observed the deposition of Au and Ag on the graphene. Therefore, we changed the reference system to a Pd/H_2 electrode. For this a palladium wire (0.5 mm diameter, 99.95%, MaTeck) was loaded with hydrogen by putting it in a 0.1 M solution of perchloric acid (Suprapur, 70%, Merck) and applying 5 V, using a gold wire as the anode. The reaction was stopped after a couple of minutes, as soon as the evolution of H_2 was visible at the Pd cathode. The as-prepared Pd wire was wrapped around the Pt wire in the cell. The electrolyte used in this configuration was a 0.1 M potassium perchlorate (Suprapur, 99.999%, Merck) solution at pH 4, where the pH was adjusted using perchloric acid.

Cyclic Voltammograms of Graphene. Cyclic voltammograms (CV) of two different graphene layers deposited on CaF_2 substrates were acquired using a Pd/H_2 reference system to test the functionality of the cell and the layers. The open-circuit potential (OCP) for these systems varied between 400 and 760 mV depending on the sample and sample history. As can be seen upon comparing Figure 4a with Figure 4b, the shape of the CVs varied between samples.

In the CVs shown in Figure 4, the current only varies slowly with varying potential close to the OCP (around 400, 700, and 500 mV in Figure 4, parts a, b, and c, respectively). These small slopes in the center result in the CVs exhibiting a shape somewhat comparable to that of a rectangle. As the CV of a capacitor has a rectangular shape,[28] this is a good indication that we are indeed contacting the graphene. The electronic properties of supported CVD grown graphene depend on the CVD growth, as grain boundaries and possibly defect sites are introduced. Furthermore, the local electronic properties are influenced by the transfer process since it is almost impossible to entirely remove physisorbed PMMA residues. Trapped or adsorbed H_2O and O_2 may further influence the electronic state of transferred graphene.[29] We quantified the Fermi level

DOI: 10.1021/acs.jpcc.9b05844
J. Phys. Chem. C 2019, 123, 24031−24038

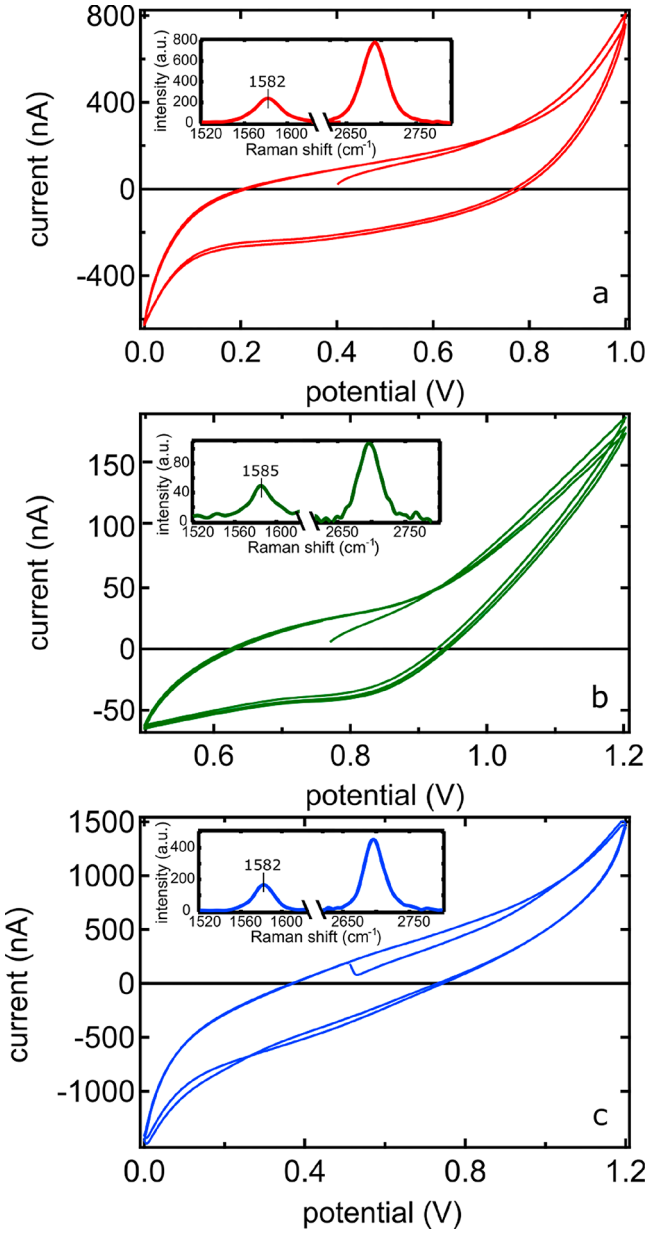

Figure 4. Cyclic voltammograms of graphene in 0.1 M $KClO_4$ at pH 4 with a Pd/H_2 reference electrode for three different graphene layers on CaF_2. All CVs were recorded in the spectro-electrochemical cell. The insets show representative Raman spectra of the respective graphene layers. The position of the G band that reflects the graphene carrier density is marked in all spectra.

of the different samples using the G band in the Raman spectra of all three samples.[25,26] In all samples, the G band is situated between 1582 and 1585 cm^{-1}, corresponding to a carrier density of $(1-9) \times 10^{11}$ cm^{-2}. The variations in the position of the G band of the Raman spectra shown in the insets of Figure 4 do not represent significant differences between the samples, as we observed similar fluctuations within each of the graphene layers. It is not completely apparent, however, how the different local environments in the different samples may affect the correlation between the OCP and the Fermi level. In addition to the described sample-to-sample variations that are inherently unavoidable, the differences in OCPs for the different samples might also be induced by the reference system used in these experiments. The reference electrode used in this study is Pd filled with H_2. After the electrode is filled with hydrogen, it is rinsed with water and mounted into the cell. The cell is subsequently closed and filled with the electrolyte solution. Depending on how long the reference electrode is kept in air during these steps and how much solution is pumped through the cell until there are no air bubbles, the state of the electrode changes slightly, which influences the OCP. The OCP, as well as the shape of the cyclic voltammograms, is further influenced by the oxygen content of the solution. The reduction of O_2 within the solution results in a tilt in the CVs. Slight variations in the oxygen content of the solution between the experiments might thus lead to different shapes of the measured cyclic voltammograms.

Sample Preparation for Static SFG Experiments. The aqueous solution was sandwiched between two windows of 2 mm thickness. The top window was placed in the cell in such a way that the graphene layer was facing the solution. The graphene substrate and all parts of the cell were rinsed with water, ethanol (absolute, Emsure) and a second time with water before assembling the cell and filling it with the aqueous solution. The H_2O used for rinsing as well as for the measurements was deionized with a Millipore unit (resistivity ≥18.2 MΩ cm). D_2O (99.9%) was obtained from Euriso-top and used as received. The acidic and basic solutions were prepared by dissolving hydrochloric acid (≥37%, Sigma-Aldrich) and sodium hydroxide (98−100%, Sigma-Aldrich) in H_2O, respectively. Sodium chloride (≥99.5%, Sigma-Aldrich) was baked at 650 °C for a couple of hours to remove organic impurities and dissolved in H_2O at the desired concentration immediately after cooling down.

SFG Experiments. The SFG experiments were performed on a setup using a Ti:sapphire regenerative amplifier (Solstice Ace, Spectra-Physics) generating 800 nm pulses with a duration of 40 fs and a repetition rate of 1 kHz. The broadband infrared pulses were generated in an optical parametric amplifier (TOPAS Prime, Spectra-Physics) with a noncollinear translation stage. The visible pulse was spectrally narrowed in a Fabry−Perot etalon (SLS Optics Ltd.), and the SFG signal was spectrally resolved and detected with a spectrograph (Acton Spectro Pro, SP-2300, Princeton Instruments) and an electron-multiplied charge couple device (emCCD) camera (ProEM 1600, Roper Scientific). All spectra were collected in ssp polarization. The signals from 100 nm gold-coated CaF_2 and SiO_2 windows, respectively, were used to normalize the spectra for the shape of the IR pulse. For the experiments, the height and tilt of the sample cell were adjusted, to match those of the gold reference, using a HeNe laser that reflected from the sample surface, directed through a pinhole and projected onto the wall. If not otherwise indicated, the power of both the IR and VIS laser pulses was reduced to 2 μJ to avoid damaging the graphene layer. Both laser pulses were weakly focused onto the sample at an angle of incidence of 33° (IR) and 37° (VIS), respectively. The spot sizes at the sample surface were estimated to have a diameter of several hundreds of micrometers. Due to the low laser power, the signal had to be acquired for at least 20 min for the signal-to-noise ratio to be sufficient. The signal-to-noise ratio could not be improved further, as the samples gradually change with time (see also below), especially during the electrochemical experiment. As such, it is not feasible to further increase the acquisition time, without averaging over effectively different samples. During the potential-controlled measurements, at

DOI: 10.1021/acs.jpcc.9b05844
J. Phys. Chem. C 2019, 123, 24031−24038

least one cyclic voltammogram (CV) was acquired before and after each SFG measurement.

RESULTS AND DISCUSSION

Static SFG Experiments. To study the hydrophobicity of graphene, we investigate the free OH SFG signal at the graphene−water interface. The water−air interface exhibits a significant spectral feature at 3700 cm^{-1} which originates from non-hydrogen-bonded groups that are dangling in air. The interface of water with hydrophobic materials, such as an octadecyltrichlorosilane (OTS) layer, has been shown to exhibit the same spectral feature.[30] The spectral feature of the dangling OH bonds can thus be used as an indicator for a hydrophobic material. Such a feature has recently been reported in an SFG simulation study, for the graphene−water interface.[6] Figure 5 shows an SFG spectrum of the

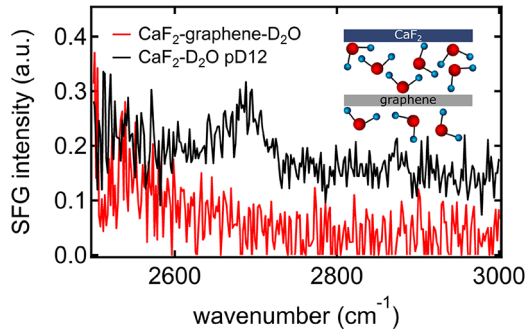

Figure 5. SFG spectra of a graphene−D_2O interface and a CaF_2−D_2O interface at pD 12. The CaF_2−D_2O spectrum is offset for clarity. Note the absence of a free OD resonance for the graphene−D_2O system, whereas the O−D stretch vibration of Ca−OD groups is clearly visible for the CaF_2−D_2O interface.

graphene−D_2O interface in the free-OD frequency region. In this spectrum, we do not observe a dangling OD signal, which is expected around 2750 cm^{-1}.[31] The spectrum of the graphene−D_2O interface is compared with a spectrum from the CaF_2−D_2O interface at pD = 12. At pD = 12, the CaF_2 surface exhibits a Ca−OD spectral feature that appears roughly 40 cm^{-1} lower than the free OD at the water−air interface.[14,32] The observation of this peak assures that the free OD could have been monitored despite the low laser powers.

The lack of a free OH signal at the graphene surface has also been reported in an experimental SFG study, where the graphene was deposited on a sapphire substrate.[33] There are two possible explanations for the absence of the free OD signal. One is that the graphene surface is not hydrophobic, and thus its interface with water does not display a free OD feature. The second possible explanation is that water molecules could be present on both sides of the graphene (see schematic inset in Figure 5—this scenario is discussed in more detail below). Please note that this schematic is just a cartoon to show the presence of water on both sides of the graphene layer and the water molecules at the graphene layer are not necessarily strictly ordered in the way indicated here. The signal from the water molecules sandwiched between the substrate and the graphene layer would then counteract the signal from the water molecules on the side of the graphene layer in contact with bulk water. In line with the second possible explanation, the presence of a free OH at the graphene water interface in simulations and its absence in experiments, has been attributed by Ohto et al.[6] to the presence of a substrate in the experiments.

Another interesting property of graphene is its proposed wetting transparency. It seems like the wetting properties of numerous materials are not significantly influenced by the presence of a layer of graphene on top of that material.[7,34] This suggests that graphene is at least partially transmitting interactions between the underlying substrate and the water molecules. We thus investigate the substrate-dependent SFG water response at a graphene monolayer. Figure 6 shows the

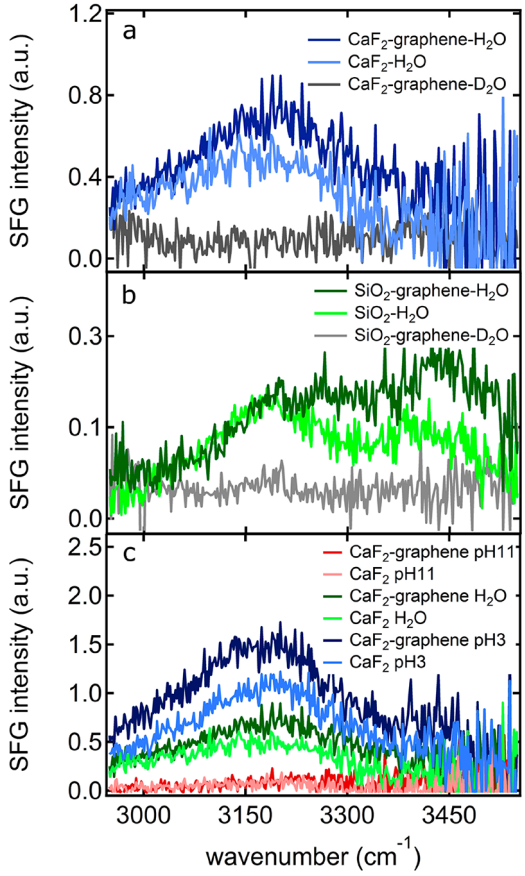

Figure 6. SFG spectra of the graphene−water interface where the graphene had been deposited on a CaF_2 (a) and a SiO_2 (b) substrate. The spectra of the respective substrate−water interface without graphene layer are also shown for comparison. The gray spectra in both panels are the nonresonant spectra of the D_2O−graphene interface in the OH vibration region. (c) pH-dependent SFG water signal at the graphene−water and CaF_2−water interface.

SFG spectra of a CVD graphene−water (H_2O) interface, where the graphene layer had been deposited on two different substrates, namely CaF_2 and SiO_2. The spectra of the water−graphene interface are compared with the spectra of the respective bare substrate-water interface. This comparison clearly shows that the shape of the SFG water response is not dominated by the graphene layer but by the underlying substrate. The gray SFG spectra in the panels a and b of Figure 6 show the SFG signal from the graphene−D_2O interface in the O−H stretch region. The fact that there is no signal for the graphene-D_2O interface at OH stretch frequencies indicates that the signal from the graphene−H_2O interface originates from interfacial water molecules and not from a nonresonant signal from graphene or the substrate. The spectral shape at

DOI: 10.1021/acs.jpcc.9b05844
J. Phys. Chem. C 2019, 123, 24031−24038

this interface is thus not dominated by nonresonant contributions from the conductive layer, which had been reported previously for other solid conductive materials.[18]

As shown below, the pH dependence of the water signal is another strong indicator that the SFG signal at the graphene–water interface is dominated by the underlying substrate. As explained in the introduction, the intensity of the SFG water signal depends on the number of oriented interfacial water molecules and the extent of their orientation. This, in turn, depends on the charge of the surface. A higher surface charge induces a higher order in the interfacial water molecules and therefore, a higher SFG signal. The water SFG signals at pH 3, neutral pH, and pH 11 are shown in Figure 6c for a graphene monolayer on CaF_2 and a bare CaF_2 surface, respectively. As expected from previous studies in literature, the water SFG signal at CaF_2 is largest for a pH 3 solution.[14,32] The water SFG spectra of the graphene–water interface appear to be very similar to the ones of the CaF_2-water interface, independent of the pH of the solution. Please note that even though the graphene water signals shown in Figure 6 all appear to be larger than the corresponding signals from the bare substrate–water interface, this is not generally the case.

Even though the graphene–water spectra do not show marked differences to the substrate–water spectra, it is evident from the raw spectra that the signal originates from a point where graphene is present. The raw SFG spectra of a graphene–water and CaF_2–water interface together with a background spectrum from the respective interface are shown in Figure 7. The background spectra are acquired by blocking

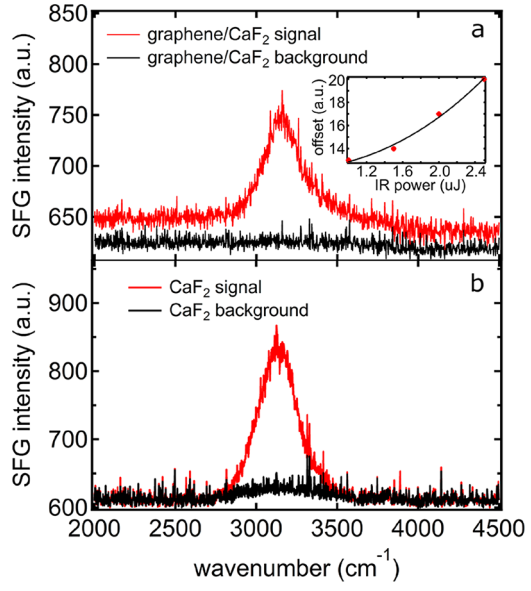

Figure 7. Raw data showing an SFG signal and background (acquired with blocked IR beam) for a CaF_2/graphene (a) and a bare CaF_2 (b) surface in contact with water. The inset in panel a shows the IR power dependence of the offset between the signal and the background on the sides of the spectra.

the infrared (but not the visible) pulse. For the CaF_2–water interface, the SFG spectrum and the background spectrum (Figure 7b) are superimposed at the low- and high-frequency side. In contrast, for the graphene–water interface, there is an offset between the signal spectrum and the background spectrum. This seems to indicate that graphene exhibits some unique frequency-independent signal originating from both the IR and VIS laser beam. As this signal extends beyond the frequency of the IR pulse, it cannot originate from any nonresonant SFG response. Thus, the offset might arise from two-photon fluorescence (IR + VIS). However, as the intensity of the offset depends nonlinearly on the power of the IR pulse (see inset in Figure 7a), the process seems to be even more complicated. In the process of analyzing the spectra, this offset is accounted for by moving the background up until it matches the signal intensity at the low- and high-frequency sides. Thus, even though the water SFG signal at the graphene surface seems to be dominated by the underlying substrate, there is some contribution from the graphene layer itself, indicating that the graphene is indeed present at the measurement spot.

All the static SFG results indicate that we are indeed able to detect a water signal at a graphene monolayer–water interface. However, the water signal seems to be dominated by the underlying substrates, despite the presence of graphene.

We have shown that our CVD graphene layers are continuous and we can contact them in our spectro-electrochemical cell to do electrochemical experiments. Since the nonresonant signal of the graphene layer does not seem to be dominating the signal, we can also apply a potential to the layer, and examine the effect of the applied potential on the interfacial water molecules.

Potential-Dependent SFG Experiments. SFG spectra of the graphene–water interface at the open circuit potential (OCP) and at an applied voltage of 1.2 V for three identically prepared graphene layers on CaF_2 are shown in Figure 8. The samples used for obtaining the potential-dependent spectra in

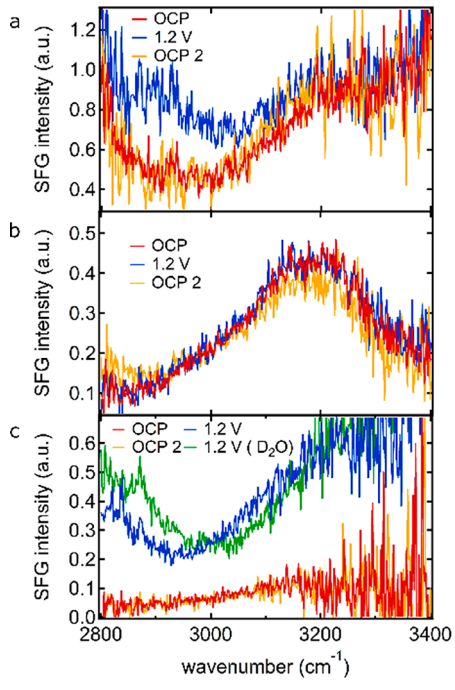

Figure 8. Water SFG spectra of the graphene–water (0.1 M $KClO_4$, pH 4) interface, with graphene on a CaF_2 substrate, at the open circuit potential (OCP), and at an applied voltage of 1.2 V, for three different samples. The OCP corresponds to a voltage of 410 mV, 760 mV, and 510 mV for the sample shown in parts a, b, and c, respectively. Panel c also shows a spectrum acquired at 1.2 V where the H_2O had been exchanged for D_2O. The yellow spectra called "OCP 2" in all three panels are spectra acquired at the OCP after the sample had been exposed to 1.2 V.

DOI: 10.1021/acs.jpcc.9b05844
J. Phys. Chem. C 2019, 123, 24031–24038

Figure 8, parts a, b, and c, correspond to those for which the CVs are shown in Figure 4, parts a, b, and c. The spectra labeled "OCP 2" in all three panels of Figure 8 were acquired after the sample had been exposed to 1.2 V, to check if the potential induced changes are reversible. Upon measuring the first sample, an additional signal at 2900 cm^{-1} appeared upon the application of 1.2 V, which disappeared again upon removing the applied voltage. The appearance of this additional signal was reversible and reproducible within the sample. That is to say, upon applying and removing the potential several times, the signal always appeared and disappeared. However, a second sample did not show any changes in the SFG signal upon changing the potential (see Figure 8b). The spectra acquired from a third sample (Figure 8c) showed a somewhat similar trend as the spectra in Figure 8a. There was also an additional signal appearing at 2900 cm^{-1}. However, for this sample, the whole signal increased as well. Furthermore, a similar change in signal was observed for that sample when the H_2O was exchanged for D_2O (green spectrum in Figure 8c). This suggests that, in this case, we were mainly inducing changes to the nonresonant SFG signal. The magnitude of the nonresonant signal is substantially smaller than that for much thicker (10−100 nm) gold or ITO films studied previously.[18,35]

The fact that there is only a small change in the water signal upon changing the surface potential quite drastically is surprising, as there are some IR studies where the change in the water signal upon changing the potential of a gold electrode is substantial.[36−38] Furthermore, the shape of the CVs changed upon exposing the layer to a certain potential for a longer period. This suggests that we were changing the layer upon exposing it to the electrolyte or upon applying a potential. In addition to the changes in CV shape, the experiments also induced an optically visible change in the graphene layers. The samples appeared more turbid in the center after the experiments. Thus, the samples were not fully stable upon treating them electrochemically. The conditions in our experiment are similar to those used for electrochemically exfoliating graphite into graphene,[27] a process during which the surface of the graphite anode is corroded at grain boundaries and edges. This might well play a role in deteriorating the graphene layers within the course of our experiments.

The experimental observation that the SFG signal change upon applying a potential seems to be negligibly small can be explained by the presence of water molecules between the graphene layer and the underlying substrate. There is always a layer of water molecules present at hydrophilic surfaces under ambient conditions.[39,40] As our CVD graphene samples are transferred onto the CaF_2 and SiO_2 substrates under ambient conditions, it is not surprising that there would be water molecules underneath the graphene. In fact, there are various reports in the literature that show the presence of water between the graphene and the substrate using AFM, XPS, Raman, and ellipsometry measurements.[41−44] The presence of water molecules on both sides of the graphene layer does not only explain the potential dependent SFG results, but also the absence of a free OD signal at the graphene surface (Figure 5) and the fact that the water SFG signal at the graphene water interface is dominated by the underlying substrate (Figure 6). The presence of water on both sides of the graphene results in a centrosymmetric, SFG-inactive system, both in the absence and in the presence of an applied potential.

CONCLUSIONS

In conclusion, we have built a spectro-electrochemical cell and have shown that we can apply a potential to a conductive graphene layer and acquire SFG spectra simultaneously. Although potential induced changes in the SFG spectra are observed, sample variations make it difficult to draw conclusions about potential-induced changes to the interfacial water structure at these surfaces. Moreover, our data indicate the presence of water on both sides of the graphene and that the substrate dominantly influences the water orientation at the surface. The interface is thus much more complex than just graphene−water, since water also intercalates in between the substrate and graphene.

In the future, it would be interesting to change the reference electrode and electrolyte once again to see whether it is possible to find a system in which the graphene layers are stable. However, it might be more promising to try different thin layer materials that might be more stable and more easily produced than graphene.

AUTHOR INFORMATION

Corresponding Author

*(M.B.) E-mail: bonn@mpip-mainz.mpg.de. Telephone: (06131) 379 536.

ORCID

A. Narita: 0000-0002-3625-522X

K. Müllen: 0000-0001-6630-8786

K.-J. Tielrooij: 0000-0002-0055-6231

E. H. G. Backus: 0000-0002-6202-0280

M. Bonn: 0000-0001-6851-8453

Present Address

#Université de Strasbourg and CNRS, ISIS, 8 allée Gaspard Monge, 67000 Strasbourg, France.

Notes

The authors declare no competing financial interest.

ACKNOWLEDGMENTS

The authors thank Helma Burg for the AFM images, Ulmas Zhumaev for his help in designing the spectroelectrochemical cell, Sheng Yang for providing us with various graphene samples and Yuki Nagata, Jonas Pfisterer, and Massoud Baghernejad for fruitful discussions. L.B.D is a recipient of a position funded by the Deutsche Forschungsgemeinschaft through the Excellence Initiative by the Graduate School Materials Science in Mainz (GSC 266). This work is funded by a DFG grant (BA 5008/3) and an ERC Starting Grant (336679). ICN2 is supported by the Severo Ochoa program from Spanish MINECO (Grant No. SEV-2017-0706). K.-J.T. acknowledges financial support through the MAINZ Visiting Professorship.

REFERENCES

(1) Surwade, S. P.; Smirnov, S. N.; Vlassiouk, I. V.; Unocic, R. R.; Veith, G. M.; Dai, S.; Mahurin, S. M. Water Desalination Using Nanoporous Single-Layer Graphene. *Nat. Nanotechnol.* **2015**, *10*, 459−464.

(2) Yang, S.; Su, Y.; Xu, Y.; Wu, Q.; Zhang, Y.; Raschke, M. B.; Ren, M.; Chen, Y.; Wang, J.; Guo, W.; et al. Mechanism of Electric Power Generation from Ionic Droplet Motion on Polymer Supported Graphene. *J. Am. Chem. Soc.* **2018**, *140*, 13746−13752.

(3) Melios, C.; Giusca, C. E.; Panchal, V.; Kazakova, O. Water on Graphene: Review of Recent Progress. *2D Mater.* **2018**, *5*, 022001.

DOI: 10.1021/acs.jpcc.9b05844
J. Phys. Chem. C 2019, 123, 24031−24038

(4) Taherian, F.; Marcon, V.; van der Vegt, N. F.; Leroy, F. What Is the Contact Angle of Water on Graphene? *Langmuir* **2013**, *29*, 1457−1465.
(5) Prydatko, A. V.; Belyaeva, L. A.; Jiang, L.; Lima, L. M. C.; Schneider, G. F. Contact Angle Measurement of Free-Standing Square-Millimeter Single-Layer Graphene. *Nat. Commun.* **2018**, *9*, 4185.
(6) Ohto, T.; Tada, H.; Nagata, Y. Structure and Dynamics of Water at Water-Graphene and Water-Hexagonal Boron-Nitride Sheet Interfaces Revealed by Ab Initio Sum-Frequency Generation Spectroscopy. *Phys. Chem. Chem. Phys.* **2018**, *20*, 12979−12985.
(7) Belyaeva, L. A.; van Deursen, P. M. G.; Barbetsea, K. I.; Schneider, G. F. Hydrophilicity of Graphene in Water through Transparency to Polar and Dispersive Interactions. *Adv. Mater.* **2018**, *30*, 1703274.
(8) Hong, G.; Han, Y.; Schutzius, T. M.; Wang, Y.; Pan, Y.; Hu, M.; Jie, J.; Sharma, C. S.; Muller, U.; Poulikakos, D. On the Mechanism of Hydrophilicity of Graphene. *Nano Lett.* **2016**, *16*, 4447−4453.
(9) Butt, H.-J.; Graf, K.; Kappl, M. *Physics and Chemistry of Interfaces*; Wiley-VCH Verlag & Co. KGaA: Weinheim, Germany, 2003.
(10) Brown, G. E., Jr.; Henrich, V. E.; Casey, W. H.; Clark, D. L.; Eggleston, C.; Felmy, A.; Goodman, D. W.; Grätzel, M.; Maciel, G.; McCarthy, M. I.; et al. Metal Oxide Surfaces and Their Interactions with Aqueous Solutions and Microbial Organisms. *Chem. Rev.* **1999**, *99*, 77−174.
(11) Asahi, R.; Morikawa, T.; Ohwaki, T.; Aoki, K.; Taga, Y. Visible-Light Photocatalysis in Nitrogen-Doped Titanium Oxides. *Science* **2001**, *293*, 269−271.
(12) Toney, M. F.; Howard, J. N.; Richer, J.; Borges, G. L.; Gordon, J. G.; Melroy, O. R.; Wiesler, D. G.; Yee, D.; Sorensen, L. B. Voltage-Dependent Ordering of Water Molecules at an Electrode-Electrolyte Interface. *Nature* **1994**, *368*, 444−446.
(13) Jena, K. C.; Covert, P. A.; Hore, D. K. The Effect of Salt on the Water Structure at a Charged Solid Surface: Differentiating Second- and Third-Order Nonlinear Contributions. *J. Phys. Chem. Lett.* **2011**, *2*, 1056−1061.
(14) Becraft, K. A.; Richmond, G. L. In Situ Vibrational Spectroscopic Studies of the CaF_2/H_2O Interface. *Langmuir* **2001**, *17*, 7721−7724.
(15) Ostroverkhov, V.; Waychunas, G. A.; Shen, Y. R. Vibrational Spectra of Water at Water/A-Quartz (0001) Interface. *Chem. Phys. Lett.* **2004**, *386*, 144−148.
(16) Yeganeh, M. S.; Dougal, S. M.; Pink, H. S. Vibrational Spectroscopy of Water at Liquid/Solid Interfaces: Crossing the Isoelectric Point of a Solid Surface. *Phys. Rev. Lett.* **1999**, *83*, 1179−1182.
(17) Tong, Y.; Lapointe, F.; Thämer, M.; Wolf, M.; Campen, K. R. Hydrophobic Water Probed Experimentally at the Gold Electrode/Aqueous Interface. *Angew. Chem., Int. Ed.* **2017**, *56*, 4211−4214.
(18) Backus, E. H. G.; Garcia-Araez, N.; Bonn, M.; Bakker, H. J. On the Role of Fresnel Factors in Sum-Frequency Generation Spectroscopy of Metal−Water and Metal-Oxide−Water Interfaces. *J. Phys. Chem. C* **2012**, *116*, 23351−23361.
(19) Brownson, D. A. C.; Banks, C. E. *The Handbook of Graphene Electrochemistry*. Springer-Verlag London Ltd.: London, 2014.
(20) Holroyd, C.; Horn, A. B.; Casiraghi, C.; Koehler, S. P. K. Vibrational Fingerprints of Residual Polymer on Transferred Cvd-Graphene. *Carbon* **2017**, *117*, 473−475.
(21) Wang, X.; Dolocan, A.; Chou, H.; Tao, L.; Dick, A.; Akinwande, D.; Willson, C. G. Direct Observation of Poly(Methyl Methacrylate) Removal from a Graphene Surface. *Chem. Mater.* **2017**, *29*, 2033−2039.
(22) Her, M.; Beams, R.; Novotny, L. Graphene Transfer with Reduced Residue. *Phys. Lett. A* **2013**, *377*, 1455−1458.
(23) Ferrari, A. C.; Meyer, J. C.; Scardaci, V.; Casiraghi, C.; Lazzeri, M.; Mauri, F.; Piscanec, S.; Jiang, D.; Novoselov, K. S.; Roth, S.; et al. Raman Spectrum of Graphene and Graphene Layers. *Phys. Rev. Lett.* **2006**, *97*, 187401.
(24) Ferrari, A. C.; Basko, D. M. Raman Spectroscopy as a Versatile Tool for Studying the Properties of Graphene. *Nat. Nanotechnol.* **2013**, *8*, 235−246.
(25) Das, A.; Pisana, S.; Chakraborty, B.; Piscanec, S.; Saha, S. K.; Waghmare, U. V.; Novoselov, K. S.; Krishnamurthy, H. R.; Geim, A. K.; Ferrari, A. C.; et al. Monitoring Dopants by Raman Scattering in an Electrochemically Top-Gated Graphene Transistor. *Nat. Nanotechnol.* **2008**, *3*, 210−215.
(26) Yan, H.; Xia, F.; Zhu, W.; Freitag, M.; Dimitrakopoulos, C.; Bol, A. A.; Tulevski, G.; Avouris, P. Infrared Spectroscopy of Wafer-Scale Graphene. *ACS Nano* **2011**, *5*, 9854−9860.
(27) Yang, S.; Lohe, M. R.; Mullen, K.; Feng, X. New-Generation Graphene from Electrochemical Approaches: Production and Applications. *Adv. Mater.* **2016**, *28*, 6213−6221.
(28) Lämmel, C.; Schneider, M.; Weiser, M.; Michaelis, A. Investigations of Electrochemical Double Layer Capacitor (EDLC) Materials - a Comparison of Test Methods. *Materialwiss. Werkstofftech.* **2013**, *44*, 641−649.
(29) Yang, G.; Li, L.; Lee, W. B.; Ng, M. C. Structure of Graphene and Its Disorders: A Review. *Sci. Technol. Adv. Mater.* **2018**, *19*, 613−648.
(30) Du, Q.; Freysz, E.; Shen, Y. R. Surface Vibrational Spectroscopic Studies of Hydrogen Bonding and Hydrophobicity. *Science* **1994**, *264*, 826−828.
(31) Bonn, M.; Nagata, Y.; Backus, E. H. G. Molecular Structure and Dynamics of Water at the Water−Air Interface Studied with Surface-Specific Vibrational Spectroscopy. *Angew. Chem., Int. Ed.* **2015**, *54*, 5560−5576.
(32) Khatib, R.; Backus, E. H. G.; Bonn, M.; Perez-Haro, M. J.; Gaigeot, M. P.; Sulpizi, M. Water Orientation and Hydrogen-Bond Structure at the Fluorite/Water Interface. *Sci. Rep.* **2016**, *6*, 24287.
(33) Singla, S.; Anim-Danso, E.; Islam, A. E.; Ngo, Y.; Kim, S. S.; Naik, R. R.; Dhinojwala, A. Insight on Structure of Water and Ice Next to Graphene Using Surface-Sensitive Spectroscopy. *ACS Nano* **2017**, *11*, 4899−4906.
(34) Rafiee, J.; Mi, X.; Gullapalli, H.; Thomas, A. V.; Yavari, F.; Shi, Y.; Ajayan, P. M.; Koratkar, N. A. Wetting Transparency of Graphene. *Nat. Mater.* **2012**, *11*, 217−222.
(35) Achtyl, J. L.; Vlassiouk, I. V.; Fulvio, P. F.; Mahurin, S. M.; Dai, S.; Geiger, F. M. Free Energy Relationships in the Electrical Double Layer over Single-Layer Graphene. *J. Am. Chem. Soc.* **2013**, *135*, 979−981.
(36) Ataka, K.; Yotsuyanagi, T.; Osawa, M. Potential-Dependent Reorientation of Water Molecules at an Electrode/Electrolyte Interface Studied by Surface-Enhanced Infrared Absorption Spectroscopy. *J. Phys. Chem.* **1996**, *100*, 10664−10672.
(37) Ataka, K.; Osawa, M. In Situ Infrared Study of Water-Sulfate Coadsorption on Gold(111) in Sulfuric Acid Solutions. *Langmuir* **1998**, *14*, 951−959.
(38) Wandlowski, T.; Ataka, K.; Pronkin, S.; Diesing, D. Surface Enhanced Infrared Spectroscopy—Au(1 1 1−20nm)/Sulphuric Acid—New Aspects and Challenges. *Electrochim. Acta* **2004**, *49*, 1233−1247.
(39) Ewing, G. E. Ambient Thin Film Water on Insulator Surfaces. *Chem. Rev.* **2006**, *106*, 1511−1526.
(40) Feibelman, P. J. The First Wetting Layer on a Solid *Phys. Phys. Today* **2010**, *63*, 34−39.
(41) Magnozzi, M.; Haghighian, N.; Miseikis, V.; Cavalleri, O.; Coletti, C.; Bisio, F.; Canepa, M. Fast Detection of Water Nanopockets Underneath Wet-Transferred Graphene. *Carbon* **2017**, *118*, 208−214.
(42) Severin, N.; Lange, P.; Sokolov, I. M.; Rabe, J. P. Reversible Dewetting of a Molecularly Thin Fluid Water Film in a Soft Graphene-Mica Slit Pore. *Nano Lett.* **2012**, *12*, 774−779.
(43) Lee, D.; Ahn, G.; Ryu, S. Two-Dimensional Water Diffusion at a Graphene-Silica Interface. *J. Am. Chem. Soc.* **2014**, *136*, 6634−6642.
(44) Li, Q.; Song, J.; Besenbacher, F.; Dong, M. Two-Dimensional Material Confined Water. *Acc. Chem. Res.* **2015**, *48*, 119−127.

DOI: 10.1021/acs.jpcc.9b05844
J. Phys. Chem. C 2019, 123, 24031−24038